THE JOURNAL OF PHYSICAL CHEMISTRY C

Article

pubs.acs.org/JPCC

A Supramolecular Amphiphile Based on Calix[4]resorcinarene and Cationic Surfactant for Controlled Self-Assembly

Sergey V. Kharlamov,*[,†] Ruslan R. Kashapov,[†] Tatiana N. Pashirova,[†] Elena P. Zhiltsova,[†] Svetlana S. Lukashenko,[†] Albina Yu. Ziganshina,[†] Aidar T. Gubaidullin,[†] Lucia Ya. Zakharova,[†] Margit Gruner,[‡] Wolf D. Habicher,[‡] and Alexander I. Konovalov[†]

[†]A.E. Arbuzov Institute of Organic and Physical Chemistry of Kazan Scientific Center, Russian Academy of Sciences, Arbuzov str. 8, 420088 Kazan, Russian Federation

[‡]Institute of Organic Chemistry, Dresden University of Technology, Mommsenstrasse 13, D-01062 Dresden, Germany

Supporting Information

ABSTRACT: A novel supramolecular system based on calix[4]resorcinarene sulfonatoalkylated at the lower rim and piperidine-methylated at the upper rim and the cationic surfactant hexadecyl-1-azonia-4-azobicyclo[2.2.2]octane bromide was investigated by methods of NMR, tensiometry, conductometry, potentiometry, dynamic light scattering, X-ray powder diffraction, and spectral probe techniques. Both types of molecules were found to self-associate in aqueous solution, with aggregates of different morphology formed. Importantly, a supramolecular amphiphilic binary system with controlled structure and binding behavior could be fabricated. At high surfactant concentration, the formation of its own aggregates takes place. In the systems with the excess of cyclophane the supramolecular amphiphiles are formed, which, in turn, self-assemble in particles with a large hydrophobic core. Thereby the structure of supramolecular species is determined by relative fractions of components and, hence, could be selectively controlled. The found properties can be used for the design of nanocontainers with the controlled cavity size.

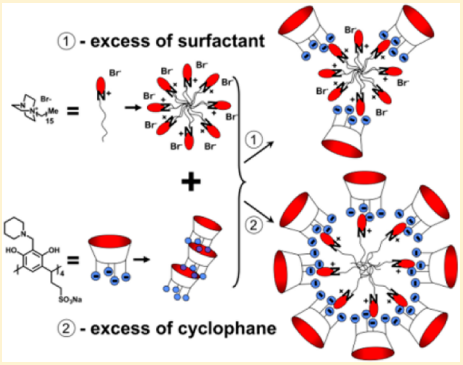

INTRODUCTION

The noncovalent design of multicomponent ensembles is a widely applied way of building the systems with new properties.[1−4] The different molecular components were self-assembled, and a lot of interesting systems were developed through this strategy, e.g., nanocontainers and nanoreactors,[5−8] molecular machines,[9−12] etc. One of the promising ideas is to use components with different structural morphology, e.g., rigid macrocycles (cucurbiturils, cyclodextrines, calixarenes, etc.) with more flexible scaffold (surfactants, polymers, etc.). In such systems noncovalent interactions lead to the fabrication of supramolecular ensembles, which combine the characteristics of composing species, but also can attain their own specificity. One of the advantages of noncovalent assembly is the avoidance of exhausting synthesis procedures. The use of compounds capable of noncovalent interactions through different mechanisms makes it possible to construct supramolecular products with different topologies and functions. From this point of view, the so-called "supramolecular amphiphiles" (SA) were developed in past few years and have shown a special significance.[4,13] In such kinds of systems the hydrophilic "head" and the hydrophobic "tail" are connected through the supramolecular interaction.[4,13,14] Biotechnological applications of these systems have been developed and studied recently, including functionalization of nanotubes,[15] design of nanoparticles,[16] gels,[17] and especially vesicles with controllable properties.[18−20] The strongest coupling in SA could be derived by electrostatic attraction. It makes the supramolecular systems relatively rigid and thermodynamically stable. Moreover, the "catanionic" type systems could be formed through a noncovalent complexation of amphiphilic anionic and cationic species. These are well-known structures with a wide range of beneficial features. They find applications in the area of drug delivery,[21] cleaning hard surfaces,[22] pharmacy,[23] as templates for nanoparticle synthesis,[24] etc. We present here the results on mixed system based on novel calix[4]resorcinarene (**1**) sulfonatoalkylated at the lower rim and piperidine-methylated at the upper rim and the cationic surfactant hexadecyl-1-azonia-4-azobicyclo[2.2.2]octane bromide (DABCO) (**2**) (Chart 1), where SA can be formed.

In our previous work, we found that aminoalkylated analogue of **1** is prone to self-associate through a "head-to-tail" pattern owing to electrostatic interactions between positively charged groups of the upper rim and negatively charged sulfonato groups of the lower one.[25] These interactions and the binding capacity of aggregates are determined by solution pH, which controls the protonation of amino groups and hence the presence of the charge at the upper rim.

Received: July 5, 2013
Revised: August 19, 2013
Published: September 3, 2013

dx.doi.org/10.1021/jp406643g | J. Phys. Chem. C 2013, 117, 20280−20288

Chart 1. Chemical Structures of 1 and 2

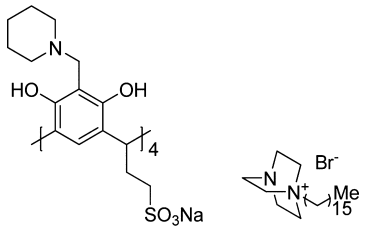

1 2

The nonalkylated precursor of **2** is widely explored in the design of efficient catalytic systems, supramolecular architectures, etc.[26−28] Self-organization of alkylated DABCOs was shown to depend on their hydrophobicity and results in the formation of both isotropic systems, i.e., micellar aggregates of different size and shape and liquid crystalline mesophases.[29−32]

In the system studied, we expect the formation of SA driven by electrostatic attractive forces. To the best of our knowledge, there are few studies of such kind of ensembles described in the literature.[33−35]

EXPERIMENTAL METHODS

Calix[4]resorcinarene (1) Synthesis Details. A mixture of 37% formaldehyde solution (0.53 mL, 9.08 mmol) and piperidine (0.89 mL, 9.08 mmol) was stirred for 1 h at 50 °C in ethanol. After that, a suspension of 2.29 g (2.27 mmol) of sodium sulfonatoethylene calix[4]resorcinarene[36] in 30 mL of ethanol was added. The reaction mixture was stirred for 48 h at 80 °C. The resulting slurry was filtered, washed with ethanol, and dried in a vacuum (2.83 g, 89.54%); mp 260−270 °C. ^{1}H NMR (D_2O, 600.13 MHz): 1.31−1.56 (broad m, 8H, $-N(CH_2CH_2)_2C\underline{H}_2$; br m, 16H, $-N(CH_2C\underline{H}_2)_2CH_2$); 2.35−2.86 (m, 8H, $-C\underline{H}_2-CH_2-SO_3Na$; m, 8H, $-CH_2-C\underline{H}_2-SO_3Na$; m, A of AB system, 8H, $-N(C\underline{H}_2CH_2)_2CH_2$); 3.11 (m, B of AB system, 8H, $-N(C\underline{H}_2CH_2)_2CH_2$), 3.97 (s, 8H, $-C\underline{H}_2-N(C_5H_{10})$; 4.48 (t, 4H, Ar−CH−Ar); 7.07 (s, 4H, ArH). ^{13}C NMR (D_2O, 150.94 MHz): 21.27, 22.88, 26.56, 33.93, 49.93, 52.43, 53.27, 106.34, 122.32, 123.95, 156.44. Anal. Calcd for $C_{60}H_{80}N_4Na_4O_{20}S_4$ %: C, 51.57; H, 5.77; N, 4.01; S, 9.18. Found: C, 51.98; H, 5.94; N, 4.10; S, 9.52. ESI-MS: m/z (%) = 1373.1 $[M^{4-} + 3Na^+]^-$, 1351.1 $[M^{4-} + 2Na^+ + H]^-$, 1329.2 $[M^{4-} + Na^+ + 2H^+]^-$, 1307.2 $[M^{4-} + 3H^+]^-$.

Chemicals. Synthesis of **2** was described elsewhere.[30] 1-Phenylazo-2-naphthol (Sudan I) (Chart 2) and D_2O were used as received (Aldrich).

Chart 2. Chemical Structure of Sudan I

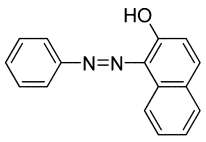

Sudan I

Measurements and Analysis. NMR experiments were performed for samples prepared in D_2O; distilled H_2O was used for all other measurements. All NMR experiments were performed on Avance-600 (Bruker, Germany) spectrometer equipped with a pulsed gradient unit capable of producing magnetic field pulse gradients in the z-direction of 56 G cm^{-1}. Chemical shifts were reported relative to HDO (4.7 ppm) as an internal standard. The DOSY spectra were acquired with the BPP-STE-LED pulse program.[37] Diffusion delay was 50 ms in all cases; bipolar gradient pulses duration was varied from 3 to 8 ms (depending on a system under investigation), 1.1 ms spoil gradient pulse (30%), and a 5 ms eddy current delay. The reported results are the mean value of multiple data points (from 2 to 6) and the standard deviations are less than 6%. Exceptions were observed only in case of low concentrations (0.1 mM) and binary systems with components ratio near the charge neutrality zone, where opacity of samples took place. All diffusion NMR measurements were performed at 25 ± 0.1 °C with a 535 L/h airflow rate in order to avoid any temperature fluctuations owing to a sample heating during the magnetic field pulse gradients. Nuclear Overhauser effects were measured by NOESY or 1D DPFGNOE methods.[38]

Electrical conductivities were measured using an InoLab Cond 720 precision conductivity meter with a graphite electrode having a cell constant of 0.475 cm^{-1} ± 1.5%. The conductance of different solutions was measured on addition of an aliquot of a known concentration of a surfactant or calix[4]resorcinarene solution to a given volume of the thermostated doubly distilled water. Reproducibility was checked for selected samples, and no significant differences were observed. All samples were studied at 25 ± 0.1 °C.

Surface tension measurements were performed using the du Nouy ring detachment method. The experimental details are described elsewhere.[39] Each data point represented the average of ca. 10−15 measurements of surface tension. Each of concentration dependence was obtained three times, and the results were within 2−3%. Besides, solutions were monitored in time, e.g., after 1, 2, and 5 days to test that they are equilibrated.

Dynamic light scattering (DLS) measurements were performed by means of the Malvern Instrument Zetasizer Nano. The measured autocorrelation functions were analyzed by Malvern DTS software and the second-order cumulant expansion methods. The effective hydrodynamic radius (R_h) was calculated according to the Einstein−Stokes relation:

$$D_S = \frac{k_B T}{6\pi\eta R_h} \quad (1)$$

in which D_S is the diffusion coefficient, k_B is the Boltzmann constant, T is the absolute temperature, and η is the viscosity. The diffusion coefficient was measured at least five times in 10 runs, so that ≥50 scans were obtained for each sample. The average error in these experiments did not exceed 4%. The solutions were filtered with Millipore filters to remove dust particles from the scattering volume. Zeta potential Nano-ZS (Malvern) with laser Doppler velocimetry and phase analysis light scattering was used for zeta potential measurement. The temperature of the scattering cell was controlled at 25 °C; the data were analyzed with the software supplied for the instrument.

Electromotive force measurements using an ion-selective electrode were used for the determination of the degree of counterion binding to aggregates (β), being the ratio of Br^- counterions and amphiphile ions in the micelles. It was calculated from the mass balance for surfactant ion and counterion at any total concentration C_t using the expression

$$\beta = \frac{C_t - [Br^-]}{C_t - \text{cmc}} \quad (2)$$

dx.doi.org/10.1021/jp406643g | J. Phys. Chem. C 2013, 117, 20280−20288

The Nernst equation described the relation between the electrode potential (ΔE) and the activity of bromide ion (a_{Br}):

$$\Delta E = -\frac{RT}{F}\log(a_{Br}) + \text{const} \quad (3)$$

where F is the Faraday constant and the ideal slope (RT/F) is 59.2 mV/equiv at 298.2 K. The measurements were performed using the ion meter I-160MI, with a Br-selective electrode ELIS-131Br and a reference electrode ESr-10101/3.0. The electromotive force (ΔE, eq 3) of the cell was measured for the sample solutions with a stepwise increasing concentration at 25 °C. Starting from the surfactant concentration of 1 mM, correction factors were used for the calculation of bromide ion concentration from the activity. Each of concentration dependence was twice or triplicate performed, and the average values were presented; the results obtained were within 2−3%.

The solubilization experiments were performed by adding an excess of the crystalline dye (Sudan I, Chart 2) to solutions. These solutions were allowed to equilibrate for about 48 h at room temperature. They were filtered, and their absorbency was measured at 500 nm (molar extinction coefficient 8700 L mol^{-1} cm^{-1}). The spectrophotometry determinations were performed on SPECORD 250 PLUS instrument (Analitic Jena, Jena Thuringia, Germany) equipped with WinAspect software at 25 °C, using a 0.1 cm path-length cell. Absorbance of the dye for each sample was obtained by subtraction of the contribution of **1** to the summary spectrum. Reproducibility was checked for selected samples, and no significant differences were observed.

The X-ray powder diffraction (XRPD) data for investigated compounds were collected on a D8 Advance diffractometer (Bruker, Germany) equipped with Vario attachment and Vantec linear PSD, using monochromated Cu Kα (1.5406 Å) radiation (40 kV, 40 mA) at 296 K; a curved Ge monochromator was employed. The powder sample of mixed **1** + **2** system for XRPD analysis was prepared by the sedimentation method. The precipitant solution was obtained by mixing **1** with **2** at a mass ratio of 1:3 in aqueous medium at room temperature. The supernatant fluid was separated by centrifuging at 6000*g* for 10 min; the deposit was washed with bidistilled water and dried in the open air. Room-temperature data were collected in the reflection mode with a flat-plate sample. The samples were loaded on a silicon plate, which was kept unmoved throughout the data collection. Patterns were recorded in the 2Θ range between 1° and 70°, in 0.008° steps, with a step time of 0.1 s. Four powder patterns were collected and summed for each sample.

RESULTS AND DISCUSSION

Single Solutions. A chemical structure of **1** was unambiguously proved by a variety of NMR correlation techniques. A cone-type (rccc) conformation was found to be the most stable for free **1** (Figure S1). In aqueous unbuffered solution of **1**, a pH of ca. 9 is spontaneously maintained due to acid−base interactions of piperidine moiety with water molecules, thereby resulting in the partial protonation of the nitrogen atoms. An additional charge character of the upper rim may originate from the intramolecular acid−base interactions of piperidine and resorcinol OH groups (pK_a of 9.15[40]). Therefore, at least the part of the moieties in the upper rim may have zwitterionic form. This assumption is in line with the absorbance at 500 nm occurring in a single **1** solution (Figure S2, pH 9), indicating the partial anionic character of resorcinol OH groups. The structure of **1** also suggests a negatively charged lower rim due to a dissociation of sulfonate groups. Thus, in analogy with aminoalkylated analogue of **1**,[25] its multicharged nature should mediate self-association processes.

Indeed, the self-diffusion coefficient D_1 decreases with the calix[4]resorcinarene concentration in aqueous media (Figure 1). Two breakpoints can be differentiated in this dependence.

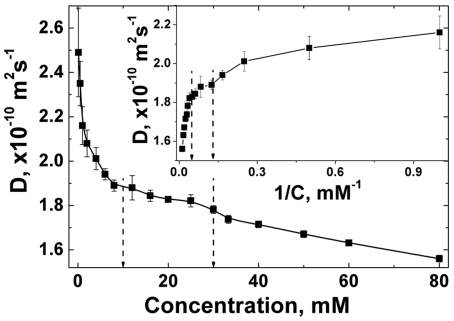

Figure 1. Dependence of the self-diffusion coefficients of **1** on its concentration (and inverse concentration, inset); D_2O, pH 9.0, 25 °C.

The first one, around 10 mM, is identified as a critical association concentration (cac_1), whereas the second critical concentration (cac_2) of 30 mM is attributed to changes in the shape of aggregates. It should be emphasized that unlike typical surfactant solutions, aggregation of calix[4]resorcinarene through electrostatic mechanism is less cooperative; e.g., the aggregation number of 8 was estimated for the dimethylaminomethylated analogue of **1**.[25] This is probably responsible for the poorly pronounced changes in solution properties of **1** upon its association. As documented in ref 41, a more marked breakpoint can be observed in the D_1 versus $1/C$ plot, which verifies the cac_1 and cac_2 values of 7 and 25 mM, respectively (Figure 1, inset).

To confirm the validity of cac in the case of such low cooperative aggregation, a complex of alternative techniques are usually applied. Taking into account the ionic structure of **1**, the specific conductivity measurements could reflect structural rearrangements in studied system. Indeed, two breakpoints are evident from conductivity (χ, μS cm^{-1}) versus concentration plot for the single **1** aqueous solution (Figure 2), i.e., 5.9 and

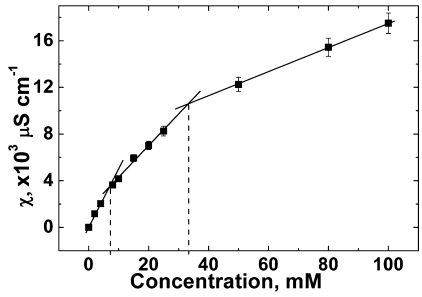

Figure 2. Dependence of the specific conductivity of the single **1** solution on its concentration; pH 9.0, 25 °C.

33.3 mM. Good linearity occurs within three sections divided by two critical points, i.e., cac_1 and cac_2, with correlation coefficients (R) being equal of 0.9962, 0.9958, and 0.9999, respectively. The lower correlation coefficients are observed if one of the break points would assume invalid, namely R = 0.9905 (first breakpoint is ignored) and R = 0.9850 (second

dx.doi.org/10.1021/jp406643g | J. Phys. Chem. C 2013, 117, 20280−20288

breakpoint is ignored) (Figure S3). This strongly supports the validity of both critical points in Figure 1.

The tensiometry method was used to test the surface activity of **1**. A marked decrease in the surface tension is shown to occur at the calix[4]resorcinarene concentration above 10 mM (Figure S4), which correlates well with NMR and conductometry results. Meanwhile, unlike typical surfactants, no significant discontinuities followed by a plateau are found in the plot.

Taking into account different charges of upper and lower rims of **1**, a "head-to-tail" scheme of the aggregate formation could be expected. In this case, nonmicellar morphology should take place; i.e., no hydrophobic core is assumed to be formed. In order to verify this point, an experiment with the dye Sudan I was performed. This dye is insoluble in water, but it could be solubilized in hydrophobic core of micelle-like aggregates, which can be detected by the appearance of absorption band of Sudan I (ca. 500 nm)[42] in the UV−vis spectrum beyond the cac_1. However, there is no absorption at any concentration of **1**, which confirms the above supposed nonmicellar structure of aggregates.

The compound **2** is a cationic surfactant, and its single solution was investigated in our earlier works, where micelle formation was demonstrated.[29−32] The dependence of the self-diffusion coefficient of **2** on its concentration has a shape typical for classical surfactants, with critical micelle concentration (cmc) being of ca. 0.8 mM (Figure S5).

Binary Solutions. The main direction of this work lies in a combination in a single system of components with principally different mechanisms of self-organization. Thus, the formation of mixed aggregates of different topologies could be expected, e.g., electrostatically or inclusive interaction driven structures. The clear solutions were observed only for the systems with the excess of one of the components, while precipitation phenomenon takes place near the charge neutrality zone (i.e., for ratios from 1:1 to 1:4 of **1** + **2** mixture). Such behavior is common in catanionic systems, where vesicles may be formed.[43,44] However, problems connected with the inhomogeneity could occur in such samples. Therefore, to determine main factors, which define the morphology of binary ensembles, and to explore the mutual influence of the components on their self-association properties, the systems with fixed concentration of one of the components were examined, while the molarity of the second specie was varied.

Aggregation of **2** in the presence of fixed amount of **1** was analyzed by alternative techniques, which would provide the reliable information, thereby rejecting valueless data. To begin with the self-diffusion coefficient measurements were carried out (Figure 3), since this technique makes it possible to monitor associative behavior of each component in the mixture. Inspection of self-diffusion coefficients shows the lower D_2 values with respect to the surfactant individual solution at the same concentrations. Thus, the strong interaction between **1** and **2** takes place. When surfactant fraction is low ([**2**] < 2 mM) the D_1 and D_2 values are almost constant. Herewith D_1 is about the same as for free **1** at 1 mM. Therefore, the most molecules of the calix[4]resorcinarene are in nonaggregated form. However, D_2 is ca. 0.5×10^{-10} m^2/s; i.e., surfactant molecules are in the associated state. It is important that this value is notably less than in individual solution of **2** at the same concentration. Hence, some kind of mixed aggregates occurs. Described behavior is observed even at [**2**] < 1 mM, i.e., before

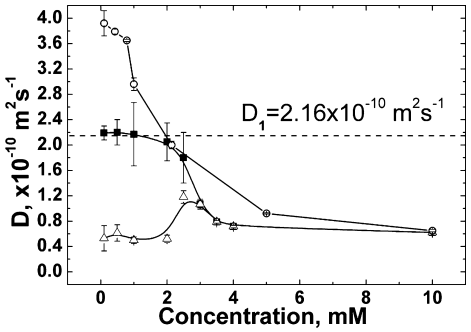

Figure 3. Dependence of D_1 (filled squares) and D_2 (open triangles) in binary mixture and D_2 in individual solution (open circles) on [**2**], [**1**] = 1 mM (D_1 of individual solution at this concentration is shown by a dashed line); D_2O, pH 9.0, 25 °C.

cmc in its single system. Therefore, **1** promotes surfactant self-assembly.

There are two possible ways of interaction between **1** and **2**: (i) inclusion of **2** into the calix[4]resorcinarene cavity; (ii) electrostatic attraction between oppositely charged lower rim of **1** and a headgroup of **2**. In the first case, notable shielding effects by aromatic cyclophane cavity should be seen. Unfortunately, a highly broadened ^1H NMR spectrum is observed for the binary system (e.g., see Figure S6). As a result, signals of a headgroup of **2** and corresponding vicinal protons could not be distinguished with confidence. Meanwhile, aliphatic protons of **2** and most of resonances of **1** are not shifted and clearly detectable; thus, self-diffusion coefficients of components were successfully measured (Figure S6). Taking into account a positive charge of an upper rim of **1** due to a protonation of piperidine groups, an electrostatic repulsion should prevent a binding of **2** by **1** using the inclusion mechanism. Therefore, the most probable mechanism of **1**−**2** complex formation is an electrostatic attraction of surfactant and low rim of the calix[4]resorcinarene. UV−vis measurements (Figure 4) are in full agreement with suggested model of

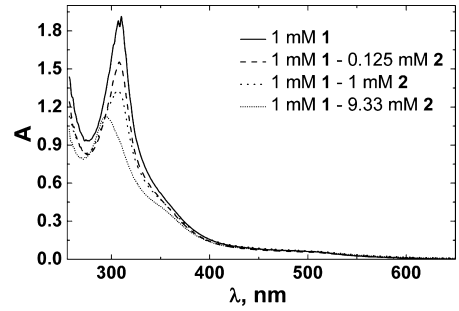

Figure 4. UV spectra of **1** + **2** mixture of different relative concentrations of components; pH 9.0, 25 °C; optical length 0.1 cm.

interaction between **1** and **2**. After addition of **2** to the single solution of **1** (1 mM) the band of calix[4]resorcinarene at 310 nm is hypsochromicaly shifted by 20 nm. This is common for the electrostatic interaction of a molecular specie with micellar structure[45] and may be followed by a counterion-induced vesicle formation,[46] as it does in the case of catanionic amphiphiles. However, the latter takes a separate investigation. Moreover, maximum intensity decreases by a factor of 1.5, which reflects the formation of organized supramolecular structures.

dx.doi.org/10.1021/jp406643g | J. Phys. Chem. C 2013, 117, 20280−20288

Thus, an interaction of **1** with **2** results in the formation of SA, in which **1** plays a role of a "head", while alkyl chain of **2** acts as a hydrophobic "tail". The full length of such SA (ca. 35 Å) is in good agreement with the hydrodynamic radius (R_h) estimation of found mixed aggregates (ca. 40 Å), which was obtained from the observed D using the Stokes−Einstein equation (see eq 1, Experimental Methods). Therefore, the formation of spherical micelle-like aggregates is the most probable.

So, the aggregation behavior of mixed system was further treated based on the suggested mechanism of aggregation. The analysis of self-diffusion data (Figure 3) in the concentration range [**2**] > 2 mM shows that D_1 value decreases, thus reflecting a greater involvement of **1** into a bound state. On the other hand, D_2 increases, which shows the rise of the relative quantity of free **2**. However, after a critical point [**2**] = 3 mM, D_2 falls again and hereinafter it is close to the values measured in individual solutions of surfactant at the same concentrations. It looks like the fraction of free **2** becomes high enough to start its own micellization process. Indeed, at [**2**] = 10 mM the R_h estimation (ca. 30 Å) is comparable to the length of surfactant monomer (ca. 25 Å), which correlates with spherical micelle formation. Moreover, $D_1 = D_2$ within this range; thus, one can conclude that molecules of **1** are adhered on surfactant micelle surface.

The assumed model of mixed association resulting in the formation of SA is well supported by potentiometric study with Br-selective electrode. First, a critical point [**2**] = 3.3 mM was also found (Figure S7a). Importantly, when [**2**] > 3.3 mM, the degree of bromide-ion binding to aggregates (β, see eq 2 in the Experimental Methods) in the binary system is noticeably less than in individual solution of **2** (Figure S7b). This probably reflects the partial replacement of bromide counterions by **1** in the surface layer of **2** within the titled concentration range.

At low concentrations (≤0.2 mM) the NMR spectroscopy exhibits poor sensitivity which prevents of analyzing the onset of aggregation, and therefore the surface tension and specific conductivity measurements were also involved to obtain reliable information about the influence of **1** on cmc of **2**. Surface tension isotherm (Figure 5a) and conductivity versus concentration plot (Figure 5b) for the binary **1**−**2** system (concentration of **1** is fixed) have a clear breakpoint at ca. 0.1 mM, which can be identified as the cmc of **2** in the presence of **1**. Thus, about 1 order decrease of cmc takes place, which is probably responsible for the low diffusion coefficients of **2** in mixed system at [**2**] < 2 mM (Figure 3). To the best of our knowledge, there are only a few examples of lowering the cmc values of simple surfactants by macrocyclic compounds in the literature.[35,47,48] Importantly, specific conductivity measurements also show the second critical point at ca. 5 mM. This is in good agreement with NMR observations (Figure 3) and assumes the change of aggregates morphology from the mixed SA based aggregates toward the micelles of **2** with adhered molecules of **1** on them.

The structure of found ensembles was probed in experiment with the hydrophobic marker Sudan I (Figure 6 and Figure S8). Here a 4 mM critical point was seen, which is in agreement with NMR and specific conductivity. Above the concentration of 4 mM the optical density of Sudan I dramatically increases from about the zero level. This correlates well with NMR data, according to which the surfactant **2** own micelles take place within this concentration region. However, at high **2** concentration the absorbency is even higher than for individual

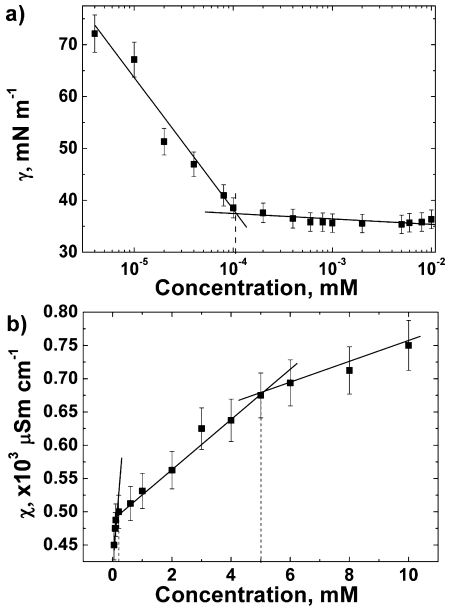

Figure 5. Surface tension (a) and specific conductivity (b) dependences on [**2**] for the binary **1**−**2** mixture, [**1**] = 1 mM; pH 9.0, 25 °C.

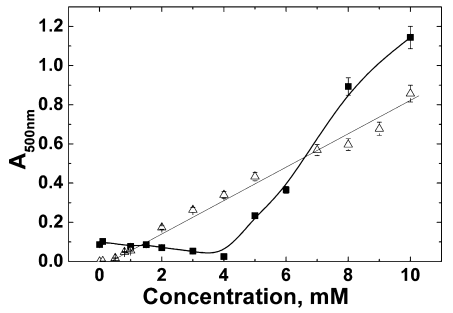

Figure 6. Optical density of Sudan I at 500 nm dependences on [**2**] in individual **2** solution (open triangles) and **1**−**2** mixture (filled squares, [**1**] = 1 mM); pH 9.0, 25 °C; optical length 0.1 cm.

solutions of surfactant. This could be a result of micelle stabilization caused by aforementioned adhering of **1** at micelle surface, which leads to reinforcement of it hydrophobic area.

It is noteworthy that a very low absorbance is observed in the concentration range [**2**] < 4 mM. At first sight, a disagreement takes place with the above treatment of the NMR results assuming the micellization of **2** promoted by **1** at low surfactant concentrations, followed by the formation of SA based mixed aggregates. On the other hand, this well correlates with the low solubilization capacity of single **2** aggregate within the concentration range close to cmc (Figure 6). Besides, the overall concentration of mixed aggregates strongly depends on [**2**], and the latter is relatively small. As a result, a quantity of solubilized dye is insignificant. From this point of view, the addition of **1** should increase the mole fraction of the SA-based mixed aggregate. In order to clarify these assumptions, binary systems with fixed [**2**] (5 mM) and varied [**1**] were also examined by the dye solubilization method (Figure 7).

As noted above, there is almost no dye solubilization for a single **1** solution at any concentration. The absorbance of Sudan I at 500 nm in pure **2** solution (5 mM) is ca. 0.45, which demonstrates that some amount of the dye is solubilized. As for the **1**−**2** mixture, the optical density concentration dependence

dx.doi.org/10.1021/jp406643g | J. Phys. Chem. C 2013, 117, 20280−20288

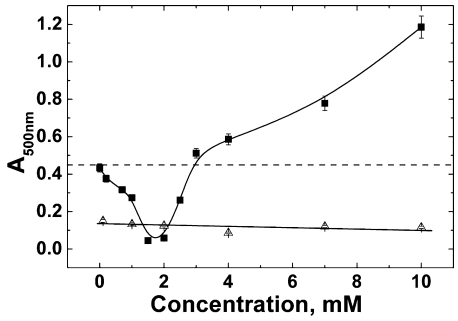

Figure 7. Optical density of Sudan I at 500 nm dependences on [**1**] in individual **1** solution (open triangles) and **1**−**2** mixture (filled squares, [**2**] = 5 mM); the corresponding optical density for individual **2** solution is shown by a dashed line; pH 9.0, 25 °C; optical length 0.1 cm.

has an extremum form. At the first stage, when relative concentration of **1** is low, the absorbance of Sudan I is expectedly close to the value for individual solution of **2** at 5 mM. Then it decreases with the rise of mole fraction of **1**, which most probably indicates that **1** interacts with **2** and takes them out from the micelles with destroying the latter. In other words, **1** plays a role of electrostatic "forceps", which nips off positively charged surfactant molecules from their own micelles and as a result causes Sudan I to leave the system.

It should seem that the excess of calix[4]resorcinarene will finally destroy micelles, and therefore, there would not be any hydrophobic areas in the sample. However, the experiment shows the pronounced rise of the observed optical density of the absorption band of Sudan I (Figure 7, [**1**] > 2 mM). Hence, the aggregates with a hydrophobic core sufficient for dye solubilization are formed. Obviously, the aforementioned detaching of surfactant molecules from their single aggregates by **1** leads to forming of **1**−**2** complexes; i.e., the SA is formed. These SAs, in turn, self-aggregate and form ensembles with large hydrophobic cavity. Thus, the above made assumption about SA-based aggregate formation is confirmed.

Taking into account the charged nature of interacting species, some additional information could be derived from zeta-potential measurements (Figure 8). Individual solutions of **2** have ca. +50 mV zeta-potential in all concentration range, which reflects overall positive charge of its aggregates. On the other hand, zeta-potential of **1** is ca. −40 mV. Therefore, an addition of the surfactant to the sample with fixed amount of **1** (1 mM) leads to a gradual charge compensation in the binary system (Figure 8a), and after charge neutrality point ([**2**] > 4 mM, see Figures 3 and 6 for comparison), the zeta-potential becomes positive. However, it is still lower than in individual solutions. This confirms the aggregation mode, when micelles of **2** takes place and their surface charge is compensated by adhered molecules of **1**, which binding degree is higher as compared to bromide counterion.

In the opposite case, when [**2**] is fixed (5 mM) (Figure 8b), another behavior of zeta-potential takes place. When fraction of **1** is low, the overall positive charge is observed. This is due to dominance of individual micelles of **2**. The increase of concentration of **1** leads to pronounced lowering of zeta-potential. This can be explained by the aforementioned "nipping" of surfactant molecules by calix[4]resorcinarene "forceps", which destroys micelles of **2**. After a critical point of [**1**] = 2 mM (see Figure 7 for comparison) zeta-potential changes its sign and becomes almost invariable. This indicates

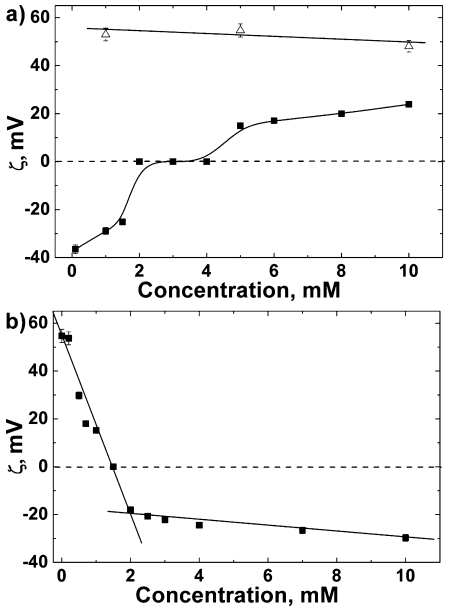

Figure 8. Zeta-potential of binary mixtures (filled squares) with fixed amount of (a) **1** (1 mM), zeta-potential of individual **2** solutions shown by open triangles, [**2**] = 0−10 mM and (b) **2** (5 mM), [**1**] = 0−10 mM; pH 9.0, 25 °C.

full destruction of surfactant micelles with simultaneous formation of SA based ensembles, with some amount of **1** being in excess.

Finally, the **1**−**2** aggregates formation was additionally supported by XRPD and DLS measurements. To verify the supramolecular complex **1**−**2** rather than the mechanical mixture formation, a comparative study of the structure of the powder sample of the mixed **1** + **2** system (see Experimental Methods for details) and starting individual substances using XRPD was carried out (Figure 9). As it has

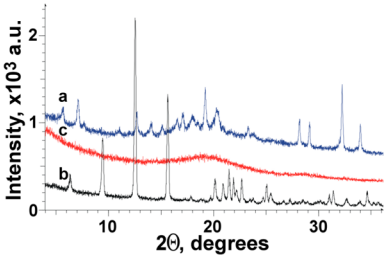

Figure 9. Experimental XRPD diffractograms of **1** (a), **2** (b), and mixed system **1** + **2** (c).

been known,[49] the powder diffraction pattern from the mechanical mixture of two crystalline compounds should be represented as the sum of the corresponding diffractograms. The results of the mixed system based on **1** and **2** investigations by XRPD are good evidence of our assumption about SA formation. Data in Figure 9 indicate that both starting compounds are crystalline substances (curves a and b). In contrast, the sample of the obtained **1** + **2** mixture is an amorphous solid and, being placed on the Si plate, produces no distinct powder diffraction pattern (curve c). Therefore, the mixed **1**−**2** supamolecular system takes place rather than their mechanical mixture.

dx.doi.org/10.1021/jp406643g | J. Phys. Chem. C 2013, 117, 20280−20288

DLS data (Figure S9) show that systems with the excess of **2** (1 mM of **1** vs 10 mM of **2**) mainly (95%) consist of particles with a hydrodynamic diameter $D_h \sim 18$ nm. This value corresponds to relatively small structures such as micelles. At the same time there is a small amount (5%) of much larger species with $D_h \sim 130$ nm, which can be attributed to SA-based mixed aggregates. In opposite, when an excess of **1** takes place (10 mM of **1** vs 5 mM of **2**) and SA-based architecture was found to arise (see above), up to 90% of particles are actually characterized by a large $D_h \sim 94$ nm, while only 5% have the size of ca. 11 nm. Therefore, the DLS method also shows two types of binary aggregates, which morphologies strongly depend on the relative fraction of components. Populations with the large size are in agreement with the above assumption on the formation of vesicles based on SA.

To summarize the data on the structural behavior of the binary **1**−**2** system, the following points should be emphasized. The reliable arguments supporting the formation of mixed aggregates are derived, which make it possible assumptions to be withdrawn on the moving forces responsible for the interactions. (i) The consistency of self-diffusion coefficient changes, and especially their closeness for the components indicates their mutual influence and their existence as a monospecie, which is verified by the XRPD data as well. (ii) A marked decrease in self-diffusion coefficients of both components with an increase in the surfactant concentration beyond critical point of ca. 3 mM (Figure 3) demonstrates that their mixed aggregation occurs, which is contributed by hydrophobic effect (i.e., by the growth of entropy due to isolating of hydrophobic hexadecyl tails from the unfavorable contacts with water). (iii) Electrostatic contributions are strongly supported by the surface charge compensation up to the neutralization in the binary system, which is evident from a zero zeta-potential in Figure 8. Besides, a marked blue shift in the UV−vis spectrum (Figure 4) occurring in the binary system and a decrease in the counterion binding (Figure S7) argue in favor of this conclusion as well. (iv) The morphology transition from the head-to-tail packing mode of the single **1** system mediated by electrostatic interactions to the micelle-like aggregates or vesicles formed by SA due to hydrophobic effect is strongly supported by the dye solubilization study which revealed a marked increase in the solubilization capacity resulting from this transition (Figures 6 and 7).

CONCLUSION

A novel supramolecular system based on calix[4]resorcinarene sulfonatoalkylated at the lower rim and piperidine-methylated at the upper rim and the cationic surfactant hexadecyl-1-azonia-4-azobicyclo[2.2.2]octane bromide were investigated. Both molecules were found to self-associate. A complex of physicochemical methods allowed independent demonstration of the formation of the two types of supramolecular structures in **1**−**2** binary systems. When the concentration of **1** is much lower with respect to **2**, the ensembles based on surfactant micelles take place. Herewith, molecules of **1** are adhered on micelle surface playing the role of counterions. In opposite, when the relative concentration of **1** is high, SAs are formed, which self-organize in mixed aggregates with a large hydrophobic domain, in which lypophilic molecules can be solubilized. The dynamic equilibrium between these two types of supramolecular structures takes place, and it could be shifted by changing the relative concentration of components of binary system. Thus, the studied mixed system can be considered as a good candidate for constructing of molecular transporters with controlled morphology and size behavior.

ASSOCIATED CONTENT

Supporting Information

2D NOESY spectrum, surface tension isotherm and solubilization ability of **1**; self-diffusion behavior of **2** and its binary solution with **1**; the electrode potential and the degree of counterion Br^- binding to aggregates in binary solutions, as well as some experimental details of the protocol used. This material is available free of charge via the Internet at http://pubs.acs.org.

AUTHOR INFORMATION

Corresponding Author

*E-mail khsergey@iopc.ru; Tel +7 (843) 2319173; Fax +7 (843) 2732253 (S.V.Kh.).

Notes

The authors declare no competing financial interest.

ACKNOWLEDGMENTS

This work was financially supported by the Russian Foundation for Basic Research (Grants 12-03-31544 and 12-03-00379) and the Russian President Scholarship (SP-6310.2013.4). This investigation was carried out in the NMR department of the Federal collective spectral analysis center for physical and chemical investigations of structure, properties, and composition of matter and materials.

ABBREVIATIONS

NMR, nuclear magnetic resonance; SA, supramolecular amphiphile; DOSY, diffusion-ordered spectroscopy; cac, critical association concentration; cmc, critical micelle concentration; DLS, dynamic light scattering; DABCO, hexadecyl-1-azonia-4-azobicyclo[2.2.2]octane bromide; XRPD, X-ray powder diffraction.

REFERENCES

(1) Lee, Y.; Ishii, T.; Cabral, H.; Kim, H.-J.; Seo, J.-H.; Nishiyama, N.; Oshima, H.; Osada, K.; Kataoka, K. Charge-conversional polyionic complex micelles−efficient nanocarriers for protein delivery into cytoplasm. *Angew. Chem., Int. Ed.* **2009**, *48*, 5309−5312.

(2) Nandan, B.; Kuila, B. K.; Stamm, M. Supramolecular assemblies of block copolymers as templates for fabrication of nanomaterials. *Eur. Polym. J.* **2011**, *47*, 584−599.

(3) Wang, C.; Wang, T.; Wang, Q. Solvent annealing assisted self-assembly of hydrogen-bonded interpolymer complexes of AB block copolymer/C homopolymer in thin film. *Polymer* **2010**, *51*, 4836−4842.

(4) Zhang, X.; Wang, C. Supramolecular amphiphiles. *Chem. Soc. Rev.* **2011**, *40*, 94−101.

(5) Kim, K. T.; Meeuwissen, S. A.; Nolte, R. J. M.; van Hest, J. C. M. Smart nanocontainers and nanoreactors. *Nanoscale* **2010**, *2*, 844−858.

(6) Kashapov, R. R.; Kharlamov, S. V.; Habicher, W. D.; Latypov, Sh. K.; Lukashenko, S. S.; Pashirova, T. N.; Zakharova, L. Ya.; Ziganshina, A. Y.; Ziltsova, E. P.; Konovalov, A. I. Novel self-assembling system based on resorcinarene and cationic surfactant. *Phys. Chem. Chem. Phys.* **2011**, *13*, 15891−15898.

(7) Zakharova, L. Ya.; Semenov, V. E.; Voronin, M. A.; Valeeva, F. G.; Ibragimova, A. R.; Giniatullin, R. Kh.; Chernova, A. V.; Kharlamov, S. V.; Kudryavtseva, L. A.; Latypov, Sh. K.; Reznik, V. S.; Konovalov, A. I. Nanoreactors based on amphiphilic uracilophanes: self-

organization and reactivity study. *J. Phys. Chem. B* **2007**, *111*, 14152−14162.
(8) Kashapov, R. R.; Pashirova, T. N.; Zhiltsova, E. P.; Lukashenko, S. S.; Ziganshina, A. Yu.; Zakharova, L. Ya. Supramolecular systems based on aminomethylated calix[4]resorcinarene and a cationic surfactant: catalysts of the hydrolysis of esters of phosphorus acids. *Russ. J. Phys. Chem. A* **2012**, *86*, 200−204.
(9) Jeon, W. S.; Ziganshina, A. Y.; Lee, J. W.; Ko, Y. H.; Kang, J.-K.; Lee, C.; Kim, K. A [2]pseudorotaxane-based molecular machine: reversible formation of a molecular loop driven by electrochemical and photochemical stimuli. *Angew. Chem., Int. Ed.* **2003**, *115*, 4231−4234.
(10) Wang, Y.; Ma, N.; Wang, Z.; Zhang, X. Photocontrolled reversible supramolecular assemblies of an azobenzene-containing surfactant with α-cyclodextrin. *Angew. Chem., Int. Ed.* **2007**, *46*, 2823−2826.
(11) Kharlamov, S. V.; Ziganshina, A. Y.; Aganov, A. V.; Konovalov, A. I.; Latypov, Sh. K. Solution structure and equilibrium of new calix[4]resorcinarene complexes−prototype of molecular machines. NMR data. *J. Inclusion Phenom. Macrocyclic Chem.* **2007**, *58*, 389−398.
(12) Kharlamov, S. V.; Ziganshina, A. Y.; Mukhitova, R. K.; Latypov, Sh. K.; Konovalov, A. I. Redox induced translocation of a guest molecule between viologen−resorcinarene and β-cyclodextrin. *Tetrahedron Lett.* **2008**, *49*, 2566−2568.
(13) Wang, C.; Wang, Zh.; Zhang, X. Amphiphilic building blocks for self-assembly: from amphiphiles to supra-amphiphiles. *Acc. Chem. Res.* **2012**, *45*, 608−618.
(14) Gattuso, G.; Notti, A.; Pappalardo, A.; Pappalardo, S.; Parisi, V. F.; Puntoriero, F. A supramolecular amphiphile from a new water-soluble calix[5]arene and n-dodecylammonium chloride. *Tetrahedron Lett.* **2013**, *54*, 188−191.
(15) Tang, Y.; Zhou, L.; Li, J.; Luo, Q.; Huang, X.; Wu, P.; Wang, Y.; Xu, J.; Shen, J.; Liu, J. Giant nanotubes loaded with artificial peroxidase centers: self-assembly of supramolecular amphiphiles as a tool to functionalize nanotubes. *Angew. Chem., Int. Ed.* **2010**, *122*, 4012−4016.
(16) Li, X.; Qi, Z.; Liang, K.; Bai, X.; Xu, J.; Liu, J.; Shen, J. An artificial supramolecular nanozyme based on β-cyclodextrin-modified gold nanoparticles. *Catal. Lett.* **2008**, *124*, 413−417.
(17) Maciollek, A.; Munteanu, M.; Ritter, H. New generation of polymeric drugs: copolymer from NIPAAM and cyclodextrin methacrylate containing supramolecular-attached antitumor derivative. *Macromol. Chem. Phys.* **2010**, *211*, 245−249.
(18) Zhang, H.; Shen, J.; Liu, Z.; Bai, Y.; An, W.; Hao, A. Controllable vesicles based on unconventional cyclodextrin inclusion complexes. *Carbohydr. Res.* **2009**, *344*, 2028−2035.
(19) Zhang, H.; Sun, L.; Liu, Z.; An, W.; Hao, A.; Xin, F.; Shen, J. pH-responsive vesicle like particles based on inclusion complexes between cyclodextrins an dimethyl orange. *Colloids Surf., A* **2010**, *358*, 115−121.
(20) Jeon, Y. J.; Bharadwaj, P. K.; Choi, S. W.; Lee, J. W.; Kim, K. Supramolecular amphiphiles: spontaneous formation of vesicles triggered by formation of a charge-transfer complex in a host. *Angew. Chem., Int. Ed.* **2002**, *41*, 4474−4476.
(21) Boudier, A.; Castagnos, P.; Soussan, E.; Beaune, G.; Belkhelfa, H.; Menager, C.; Cabuil, V.; Haddioui, L.; Roques, C.; Rico-Lattes, I.; Blanzat, M. Polyvalent catanionic vesicles: exploring the drug delivery mechanisms. *Int. J. Pharm.* **2011**, *403*, 230−236.
(22) Malmsten, M.; Lindman, B. Ellipsometry studies of cleaning of hard surfaces. Relation to the spontaneous curvature of the surfactant monolayer. *Langmuir* **1989**, *5*, 1105−1111.
(23) Bramer, T.; Dew, N.; Edsman, K. Pharmaceutical applications for cationic mixtures. *J. Pharm. Pharmacol.* **2007**, *59*, 1319−1334.
(24) Hentze, H.-P.; Raghavan, S. R.; McKelvey, C. A.; Kaler, E. W. Silica hollow spheres by templating of catanionic vesicles. *Langmuir* **2003**, *19*, 1069−1074.
(25) Korshin, D. E.; Kashapov, R. R.; Murtazina, L. I.; Mukhitova, R. K.; Kharlamov, S. V.; Latypov, Sh. K.; Ryzhkina, I. S.; Ziganshina, A. Y.; Konovalov, A. I. Self-assembly of an aminoalkylated resorcinarene in aqueous media: host−guest properties. *New J. Chem.* **2009**, *33*, 2397−2401.
(26) Li, J.-H.; Hu, X.-C.; Xie, Y.-X. Polymer-supported DABCO−palladium complex as a stable and reusable catalyst for room temperature Suzuki−Miyaura cross-couplings of aryl bromides. *Tetrahedron Lett.* **2006**, *47*, 9239−9243.
(27) Song, Y.; Ke, H.; Wang, N.; Wang, L.; Zou, G. Baylis−Hillman reaction promoted by a recyclable protic-ionic-liquid solvent−catalyst system: DABCO−AcOH−H_2O. *Tetrahedron* **2009**, *45*, 9086−9090.
(28) Ch, R.; Tyagi, M.; Patil, P. R.; Kartha, K. P. R. DABCO: an efficient promoter for the acetylation of carbohydrates and other substances under solvent-free conditions. *Tetrahedron Lett.* **2011**, *52*, 5841−5846.
(29) Gaisin, N. K.; Gnezdilov, O. I.; Pashirova, T. N.; Zhiltsova, E. P.; Lukashenko, S. S.; Zakharova, L. Ya.; Osipova, V. V.; Dzhabarov, V. I.; Galyametdinov, Yu. G. Micellar and liquid-crystalline properties of bicyclic fragment-containing cationic surfactant. *Kolloid. Zh.* **2010**, *6*, 755−761.
(30) Pashirova, T. N.; Zhil'tsova, E. P.; Kashapov, R. R.; Lukashenko, S. S.; Litvinov, A. I.; Kadirov, M. K.; Zakharova, L. Ya.; Konovalov, A. I. Supramolecular systems based on 1-alkyl-4-aza-1-azoniabicyclo[2.2.2]octane bromides. *Russ. Chem. Bull.* **2010**, *59*, 1745−1752.
(31) Zakharova, L. Y.; Gaysin, N. K.; Gnezdilov, O. I.; Bashirov, F. I.; Kashapov, R. R.; Zhiltsova, E. P.; Pashirova, T. N.; Lukashenko, S. S. Micellization of alkylated 1.4-diazabicyclo[2.2.2]octane by nuclear magnetic resonance technique using pulsed gradient of static magnetic field. *J. Mol. Liq.* **2012**, *167*, 89−93.
(32) Zhiltsova, E. P.; Pashirova, T. N.; Kashapov, R. R.; Gaisin, N. K.; Gnezdilov, O. I.; Lukashenko, S. S.; Voloshina, A. D.; Kulik, N. V.; Zobov, V. V.; Zakharova, L.Ya.; Konovalov, A. I. Alkylated 1,4-diazabicyclo[2.2.2]octanes: Self-association, catalytic properties, and biological activity. *Russ. Chem. Bull.* **2012**, *61*, 113−120.
(33) Kabanov, A. V.; Bronich, T. K.; Kabanov, V. A.; Yu, K.; Eisenberg, A. Spontaneous formation of vesicles from complexes of block ionomers and surfactants. *J. Am. Chem. Soc.* **1998**, *120*, 9941−9942.
(34) Xing, Y.; Wang, Ch.; Han, P.; Wang, Zh.; Zhang, X. Acetylcholinesterase responsive polymeric supra-amphiphiles for controlled self-assembly and disassembly. *Langmuir* **2012**, *28*, 6032−6036.
(35) Basilio, N.; Garcia-Rio, L. Sulfonated calix[6]arene host−guest complexes induce surfactant self-Assembly. *Chem.—Eur. J.* **2009**, *15*, 9315−9319.
(36) Kobayashi, K.; Asakawa, Y.; Kato, Y.; Aoyama, Y. Complexation of hydrophobic sugars and water with tetrasulfonate derivatives of recorcinol cyclic tetramer having a polyhydroxy aromatic cavity: importance of guest−host CH-π interactions. *J. Am. Chem. Soc.* **1992**, *114*, 10307−10313.
(37) Wu, D.; Chen, A.; Johnson, C. S., Jr. An improved diffusion-ordered spectroscopy experiment incorporating bipolar-gradient pulses. *J. Magn. Reson., Ser. A* **1995**, *115*, 260−264.
(38) Stott, K.; Keeler, J.; Van, Q. N.; Shaka, A. J. One-dimensional NOE experiments using pulsed field gradients. *J. Magn. Reson.* **1997**, *125*, 302−324.
(39) Zakharova, L.; Valeeva, F.; Zakharov, A.; Ibragimova, A.; Kudryavtseva, L.; Harlampidi, H. Micellization and catalytic activity of the cetyltrimethylammonium bromide-Brij 97-water mixed micellar system. *J. Colloid Interface Sci.* **2003**, *263*, 597−605.
(40) Gawron, O.; Duggan, M.; Grelechi, C. J. Manometric determination of dissociation constants of phenols. *Anal. Chem.* **1952**, *24*, 969−970.
(41) Jansson, M.; Stilbs, P. Organic counterion binding to micelles. Effects of counterion structure on micellar aggregation and counterion binding and location. *J. Phys. Chem.* **1987**, *91*, 113−116.
(42) Tehrani-Bagha, A. R.; Singh, R. G.; Holmberg, K. Solubilization of two organic dyes by cationic ester-containing gemini surfactants. *J. Colloid Interface Sci.* **2012**, *376*, 112−118.
(43) Francisco, V.; Basilio, N.; Garcia-Rio, L.; Leis, J. R.; Maques, E. F.; Vázquez-Vázquez, C. Novel catanionic vesicles from calixarene and single-chain surfactant. *Chem. Commun.* **2010**, *46*, 6551−6553.

(44) Segota, S.; Heimer, S.; Tezak, D. New catanionic mixtures of dodecyldimethylammonium bromide/sodium dodecylbenzenesulphonate/water I. Surface properties of dispersed particles. *Colloids Surf., A* **2006**, *274*, 91−99.
(45) Lu, Q.; Gu, J.; Yu, H.; Liu, C.; Wang, L.; Zhou, Y. Study on the inclusion interaction of p-sulfonated calix[*n*]arenes with Vitamin K3 using methylene blue as a spectral probe. *Spectrochim. Acta, Part A* **2007**, *68*, 15−20.
(46) Reichardt, C. Pyridinium-N-phenolate betaine dyes as empirical indicators of solvent polarity: Some new findings. *Pure Appl. Chem.* **2008**, *80*, 1415−1432.
(47) Quintela, P. A.; Reno, R. C. S.; Kaifer, A. E. Cryptand 222 complexation of anionic surfactant counterions: drastic decrease of the cmc of sodium dodecyl and sodium decyl sulfates. *J. Phys. Chem.* **1987**, *91*, 3582−3585.
(48) Evans, D. F.; Sen, R.; Warr, G. G. Structural changes in sodium dodecyl sulfate micelles induced by using counterion complexation by macrocyclic ligands. *J. Phys. Chem.* **1986**, *90*, 5500−5502.
(49) Guinier, A. *X-ray Diffraction in Crystals, Imperfect Crystals, and Amorphous Bodies*; Courier Dover Publications: Toronto, Canada, 1994.